Comparison of 240 ka long organic carbon and carbonate records along a depth transect in the Timor Sea: Primary signals versus preservation changes

Wei Liu, François Baudin, Eva Moreno, Fabien Dewilde, Nicolas Caillon, Nianqiao Fang, Franck Bassinot

AGU PUBLICATIONS

Paleoceanography

RESEARCH ARTICLE
10.1002/2013PA002539

Key Points:
- Corg and carbonate records are studied along a depth transect
- Spectral analyses show differences between the three studied sites
- Differences are discussed in terms of changes in bottom water chemistry

Correspondence to:
F. Baudin,
francois.baudin@upmc.fr

Citation:
Liu, W., F. Baudin, E. Moreno, F. Dewilde, N. Caillon, N. Fang, and F. Bassinot (2014), Comparison of 240 ka long organic carbon and carbonate records along a depth transect in the Timor Sea: Primary signals versus preservation changes, *Paleoceanography*, *29*, 389–402, doi:10.1002/2013PA002539.

Received 25 JUL 2013
Accepted 23 APR 2014
Accepted article online 20 APR 2014
Published online 21 MAY 2014

Comparison of 240 ka long organic carbon and carbonate records along a depth transect in the Timor Sea: Primary signals versus preservation changes

Wei Liu[1,2], François Baudin[1], Eva Moreno[3,4], Fabien Dewilde[5], Nicolas Caillon[5], Nianqiao Fang[2], and Franck Bassinot[5]

[1]ISTEP, UMR 7193, Sorbonne Universités, UPMC Université Paris 6, CNRS, Paris CEDEX 05, France, [2]Department of Ocean, China University of Geosciences, Beijing, China, [3]MNHN, CNRS, UMR 7207 CR2P, Paris, France, [4]Now at MNHN, CNRS, UMR 7193 ISTEP, Paris, France, [5]CNRS, CEA, UMR 1572 LSCE, Gif-sur-Yvette, France

Abstract Total organic carbon (TOC) and calcium carbonate ($CaCO_3$) records from different water depths in the Timor Sea (NE Indian Ocean) are compared in order to better reconstruct past changes in pelagic productivity, highlight the impact of preservation at depth, and unravel the interplay of organic carbon and carbonate sedimentation. New data are presented for core MD01-2376 located at 2376 m depth. These results are compared, over the last 240 ka, with published data on two neighboring cores (MD01-2378, 1783 m and MD98-2166, 3875 m). TOC fluctuations show strong glacial/interglacial variations and Milankovitch-type oscillations (i.e., dominant frequencies centered on the 100, 41, and 23 ka bands), with an enrichment during cold periods that reflects an increase in primary productivity as well as a lesser decomposition of organic matter with depth. During interglacials, TOC values are lower and show a stronger gradient with depth of deposition than during glacials. This suggests an overall better ventilation of deepwater masses and a steeper vertical gradient in the oxygen content, possibly associated to the upward extension of the oxygen-rich deep waters relative to the glacial situation. Temporal fluctuations in the $CaCO_3$ records do not show such a glacial-interglacial pattern but reveal precession- and obliquity-related oscillations. Fluctuations in the 19–23 ka bands are only observed in the shallowest core, while fluctuations in the 41 ka band are clearly expressed in the two deepest cores, suggesting that this signal is more directly related to changes in carbonate preservation at the seafloor.

1. Introduction

The study of piston core MD01-2378 retrieved at 1783 m of water depth in the Timor Sea (Indonesian Archipelago) suggests that marine productivity in this area fluctuated with a clear precession cycle, superimposed on a long-term 100 ka glacial/interglacial oscillations [*Holbourn et al.*, 2005]. By contrast, in nearby core MD98-2166 located at a much deeper water depth (3875 m), both the total organic content (%TOC) and the $\%CaCO_3$ records show a strong 41 ka cycle, with the precession signal being of secondary importance [*Moreno et al.*, 2008]. This strong obliquity imprint was interpreted as reflecting the influence of higher latitudes through past changes in deepwater ventilation and saturation with respect to carbonates.

This comparison of *Holbourn et al.* [2005] and *Moreno et al.* [2008] results clearly emphasizes the role of early diagenesis and bottom water chemistry in preserving or modifying the initial productivity signal in the Indonesian area. This stress out the importance of studying depth transects in order to confidently separate primary productivity signals from postdepositional modifications. In order to better reconstruct past changes in pelagic productivity, estimate the impact of preservation at the seafloor, and unravel the complex interplay of organic carbon and carbonate sedimentation in the Indonesian Archipelago, the present paper is aimed at comparing TOC and $CaCO_3$ records from different water depths in the Timor Sea. It presents new data from core MD01-2376 located at 2376 m in the Timor Sea and compares them, over the last 240 ka, with published data obtained on the shallower core MD01-2378 (1783 m) and the deeper core MD98-2166 (3875 m).

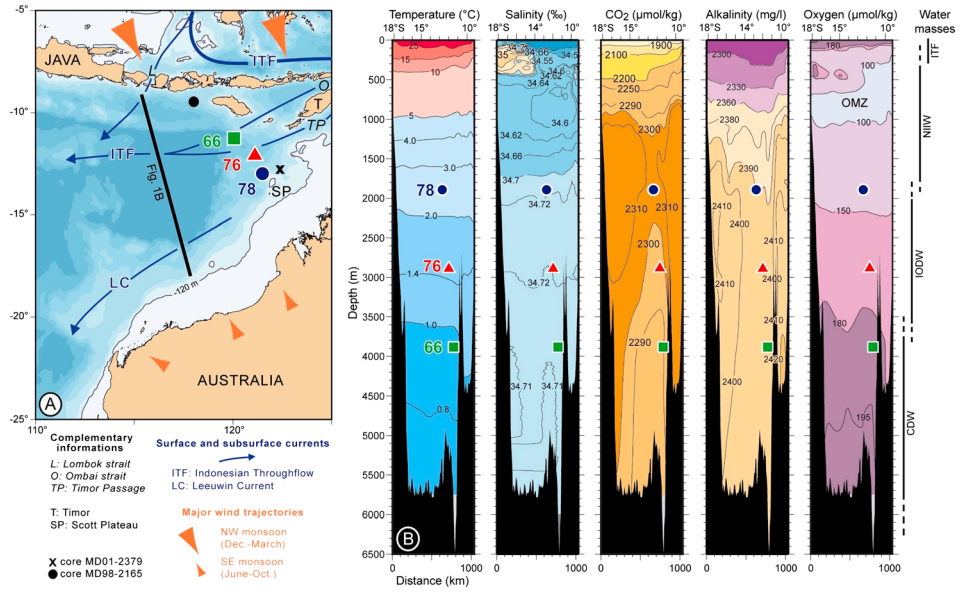

Figure 1. (a) Bathymetry of the Timor Sea in northeastern Indian Ocean and the location of the three studied cores. The bold line corresponds to the isoline 120 m, more or less equivalent to the paleocoastline during the Last Glacial Maximum (19–21 cal ka B.P.). The blue arrows indicate the main flows for the Indonesian Throughflow (ITF) and the Leeuwin Current. The orange arrows indicate the major wind trajectories during the two monsoon periods. Additional cores discussed in the text are located using black symbols. (b) Depth profiles of temperature (in °C), salinity (in ‰), total CO_2 (in µmol/kg), alkalinity (in mg/l), and oxygen content (in µmol/kg) obtained in August 1989 (during the peak of the southeast monsoon) along the Australia-Bali MD62 "JADE" IR6C section (solid line on Figure 1a) located westward to the studied sites [*Fieux et al.*, 1994]. Redrawn from World Ocean Circulation Experiment Atlas volume 4: Indian Ocean (http://www-pord.ucsd.edu/whp_atlas/indian_index.html). The bathymetry of the three studied cores is projected on these profiles. OMZ: oxygen minimum zone. On the right reported the main water masses, ITF: Indonesian Throughflow, NIIW: North Indian Intermediate Water, IODW: Indian Ocean Deep Water, and CDW: Circumpolar Deep Water.

2. Environmental Settings and Sedimentation in the Timor Sea

2.1. Modern Climatic and Hydrographic Settings

The Indonesian Archipelago (also known as the "Marine Continent") [*Ramage*, 1968] is located between two major continental masses: the Asian continent in the Northern Hemisphere and Australia in the Southern Hemisphere. Due to this particular location, the dominant climatic feature over the Indonesian region is a monsoon regime associated to the N-S displacement of the Intertropical Convergence Zone and the resulting seasonal changes in precipitation and wind direction [*Matsumoto*, 1992; *Tapper*, 2002; *Wang et al.*, 2004; *Wheeler and McBride*, 2005], with dry southeast winds blowing during boreal spring and summer and humid northwest winds bringing intense precipitation during austral summer.

The Indonesian Archipelago lies at the heart of the Indo-Pacific Warm Pool, which extends from the western Pacific to the eastern Indian Ocean and from the southern South China Sea to northern Australia. The wind stress between the Pacific and Indian Oceans maintains a sea level height difference between these two oceanic basins, leading to a net inflow of water into the Indian Ocean known as the Indonesian Throughflow (ITF) [*Hirst and Godfrey*, 1993; *Bray et al.*, 1996]. The ITF extends from the surface to ~400 m of water depth. The net volume of water transported to the Indian Ocean ranges between 10 and 15 sverdrup [*Sprintall et al.*, 2009]. It flows into the Indian Ocean through numerous shallow passages between islands and three major straits: Lombok, Ombai, and the Timor Passage (Figure 1a). The Timor Passage alone represents about 50% of the total ITF flow [*Gordon et al.*, 2010]. During the Last Glacial Maximum (LGM), wide areas of northwestern Australia and Indonesian Archipelago shelves were exposed. Consequently, the Timor Passage narrowed, and other ITF outlets were closed or restricted (see −120 m bathymetric contour line on Figure 1a). It has been suggested that oceanic heat transport by the upper ITF halved during the LGM compared to the present day [*Kuhnt et al.*, 2004].

Usually, the warm pool is defined as the region where the sea surface temperature is higher than 28°C [*Yan et al.*, 1992] or 29°C [*McPhaden and Picaut*, 1990]. Low salinities in the Timor Sea (<34 practical salinity unit (psu))

result from the influx of ITF waters and from the local excess of precipitation over evaporation [*Fieux et al.*, 1994] (Figure 1b). At depths, the "North Indian Intermediate Water" (NIIW) is characterized by a salinity maximum between 150 and 450 m, resulting from the excess of evaporation over precipitation in the latitudinal band 25°S–35°S [*Fieux et al.*, 1994]. A level of oxygen maximum is found between 350 m and 600 m of water depth (dissolved O_2 content around 190 μmol/kg; Figure 1b). This oxygenated water mass results from deep vertical convection in the southern Indian Ocean. An oxygen minimum zone (OMZ) develops below, between 600 and 1100 m, with values lower than 100 μmol/kg (Figure 1b). Below 1400 m, the water that enters the Timor Sea from the Indian Ocean is characterized by a high salinity and high-oxygen content. The salinity maximum of this "Indian Ocean Deep Water" (IODW) is found at about 2400 m with values around 34.7 psu. Deeper, the salinity is more stable toward the bottom, and the oxygen content continues to increase up to 195 μmol/kg, which marks the influence of the younger and colder "Circumpolar Deep Water" (CPDW; Figure 1b).

2.2. Past Changes in Pelagic Productivity in the Timor Sea

Today, apart from local upwelling cells developing seasonally near Indonesian islands, the Timor Sea area is globally characterized by a low, annual primary productivity (~100 g C m^{-2} a^{-1}) [*Antoine et al.*, 1996] due to the warm and low-salinity surface waters, which stabilize the upper ocean structure and restrict upper water mixing [*Gagan et al.*, 2004]. Past productivity changes reconstructed from benthic foraminifer assemblages in core MD01-2378 show (i) the dominance of an ~100 ka periodicity characterized by stronger productivity during glacials and (ii) the superimposition of a clear ~23 ka cycle, which suggests the influence of monsoon winds on upper layer mixing [*Holbourn et al.*, 2005].

Evidence suggests that the thermocline was shallower in the Timor Passage during glacial periods, when surface ITF flow was reduced [e.g., *Kuhnt et al.*, 2004; *Holbourn et al.*, 2005, 2011; *Murgese and De Deckker*, 2005]. This reduction of surface ITF flow and the thermocline shallowing may have facilitated wind-driven mixing and the increase of glacial productivity in the Timor Sea [*Xu et al.*, 2006, 2008]. In addition, mixing of surface waters might have been also facilitated by a decrease of monsoon precipitations. Paired $\delta^{18}O$ and Mg/Ca analyses on planktonic *Globigerinoides ruber* shells picked from nearby cores MD98-2165 and MD01-2378 indicate that surface water $\delta^{18}O_{sw}$ were heavier at the LGM than during the Holocene [*Levi et al.*, 2007; *Xu et al.*, 2008; *Zuraida et al.*, 2009], suggesting a decrease in precipitations and the net atmospheric export of water to higher latitudes. Drier glacial conditions over most of Indonesia and northern Australia are consistent with palynological evidence [i.e., *Kershaw et al.*, 2003].

On long time scales, the close match between Timor Sea precession-related changes in productivity and austral summer insolation (December 25°S) suggests a direct link between the productivity and the strength of NW monsoon winds [*Holbourn et al.*, 2005]. It is not clear however whether those long term changes in NW winds primarily respond to the insolation over Australia or if they reflect a transequatorial flow from the Northern Hemisphere and are therefore remotely linked to the strength of the Asian winter monsoon. The precession signature is complex however in core MD01-2378. Precession-related oscillations are strongly imprinted in the changes of benthic foraminifer assemblages but are not observed in the TOC and chlorine records. In order to explain this difference, *Holbourn et al.* [2005] suggested that oxidative degradation of organic matter at the seafloor might have smeared out the precession variability recorded in the organic-based productivity proxies.

Obliquity-related oscillations are only weakly imprinted in core MD01-2378 productivity records. They show up in the benthic foraminifer record and are also present—although weakly—in the chlorine record (at the limit of the 80% confidence interval), but they are not observed in the TOC record. By contrast, the TOC record from the nearby, deeper core MD98-2166 (3875 m) shows a well-defined obliquity-related cycle [*Moreno et al.*, 2008] superimposed on a strong ~100 ka signal, with only a weak precession contribution. The obliquity signal is also clearly expressed in the $CaCO_3$ record. Differences in the power spectra of cores MD01-2378 and MD98-2166 were interpreted as reflecting the effects of past changes in bottom water chemistry on early diagenetic processes. In addition, Rock–Eval analyses and palynofacies studies performed on core MD98-2166 also showed that part of the organic carbon could be of terrestrial origin, especially during glacial periods. This led *Moreno et al.* [2008] to suggest that TOC fluctuations may not only reflect changes of marine productivity and/or preservation at the seafloor but could also partly reflect changes in the supply of terrestrial material.

3. Material and Methods

In order to compare %TOC and %$CaCO_3$ variations at different water depths in the Timor Sea, the present study focuses on three cores recovered using the CALYPSO giant piston corer of R/V *Marion Dufresne* at water depths ranging from ~1800 to 3900 m (Figures 1a and 1b). Core MD98-2166 (11.577°S, 120.275°E; 3875 m of water depth; and 34.76 m long) was recovered in a small basin during the IMAGES IV MD111 cruise in June–July 1998 and is located at the water depth near the boundary between Indian Ocean Deep Water (IODW) and Circumpolar Deep Water (CPDW). Data used here are from *Moreno et al.* [2008]. Core MD01-2378 (13.082°S, 121.788°E; 1783 m of water depth; and 40.73 m long) was recovered at the northwestern margin of the Scott Plateau during the IMAGES VII MD122 (WEPAMA) cruise in May 2001. This site is located in the upper part of the IODW (Figure 1b). Data used in the present paper are from *Holbourn et al.* [2005]. Data from core MD01-2376 (12.314°S, 121.192°E; 2906 m of water depth; and 27.90 m long), recovered during same IMAGES VII cruise, are presented for the first time. This site lies underneath the main outflow of the ITF in the Timor Sea and within the IODW.

Visual examination and smear slide observations (Pierre-Jean Gianessini, Muséum National d'Histoire Naturelle (MNHN, Paris), personal communication) indicate that sediments from core MD01-2376 are calcareous oozes (20–45%) rich in biogenic silica (10–30%), with a strong contribution of clay minerals (25–40%) and organic matter as a subordinate component. The color of sediments varies from light olive gray to grayish olive, and bioturbation is present throughout the core. Approximately 1 cm thick slices of sediment were collected at a 10 cm interval along core MD01-2376 from 30 cm down to 2790 cm (256 samples). The $\delta^{18}O$ was measured at the Laboratoire des Sciences du Climat et de l'Environnement (LSCE, Gif-sur-Yvette) on the planktonic foraminifera *Globigerinoides ruber* (white, in a strict sense) picked from the 250–315 μm size fraction. Stable isotopes were measured using a Finnigan Δ + mass spectrometer. The $\delta^{18}O$ was calculated versus Vienna Peedee belemnite through calibration to the National Bureau of Standards 19 calcite standard [*Coplen*, 1988]. The mean external reproducibility (1σ) of carbonate standards is ±0.05‰.

Five ^{14}C dates were obtained through accelerator mass spectrometry at the ARTEMIS facility (Saclay, France) on selected *G. ruber* + *G. sacculifer*. Calendar ages were calculated using the program Calib 6.0 [*Stuiver et al.*, 1998] and the MARINE09 and corrected from reservoir effects using the global ocean average ~400 years adjusted using a local correction factor Δ*R* [*Stuiver and Braziunas*, 1993]. The estimated value of Δ*R* is 70 ± 70 years based on modern ^{14}C data obtained in surface waters northwest of Australia by *O'Connor et al.* [2010].

$CaCO_3$ content along core MD01-2376 was determined at Muséum National d'Histoire Naturelle (MNHN, Paris) using a carbonate bomb, while total carbon (TC) content was measured using a LECO IR212 at Université Pierre et Marie Curie (Paris). Total organic carbon content (%TOC) was calculated as TOC = TC − IC (inorganic carbon) with IC = $CaCO_3$/8.33, assuming that all inorganic carbon is pure calcite. The same procedure had been used for core MD98-2166 [*Moreno et al.*, 2008], whereas organic carbon and carbonate contents for core MD01-2378 were measured using a carbon, hydrogen, and nitrogen-oxygen (CHN-O) Carlo Erba analyzer [*Holbourn et al.*, 2005]. It is known that carbonate contents determined using CHN elemental analyses are overestimated compared to those determined with a carbonate bomb [*Dunn*, 1980]. The fact that we are dealing with a constant bias is clearly attested by the striking similarity between the three %$CaCO_3$ records obtained with two different methods (Figure 4). Based on Dunn's observations and our own expertise, we estimated the offset of CHN data relative to carbonate bomb data to be in the order of +7%. We plotted in Figure 4 the original %$CaCO_3$ data of core MD01-2378 [*Holbourn et al.*, 2005] together with the corrected carbonate curve (−7%). In the following discussion, we will refer to the corrected %$CaCO_3$ data.

We counted the proportion of foraminiferal fragments in the >150 μm size fraction, a well-known proxy used for documenting changes of preservation/dissolution of pelagic carbonate material [i.e., *Thunell*, 1976; *Le and Shackleton*, 1992; *Bassinot et al.*, 1994]. Each sample was carefully split in order to reduce the amount of particles to about 500–700 without systematic biases. These particles were all dispersed randomly on a counting tray, and a total of ~300 particles were counted, with replicate analyses performed for each sample. The fragmentation percentage is calculated as

$$\text{fragments}\% = (\text{number of foraminifer fragments})/(\text{number of fragments} + \text{whole foraminifer shells}) * 100$$

To extract the significant periodicities over the studied time interval, spectral analyses were performed using the RedFit software [*Schulz and Mudelsee*, 2002]. Some differences can be observed when using different windows or time intervals. We used the followed settings: OFAC = 6, HIFAC = 1, *n*50 = 1, and a rectangular window.

Table 1. AMS ^{14}C Datings for Core MD01-2376[a]

Sample Laboratory Number	Core Depth (cm)	Dated Foram Species	Uncorrelated ^{14}C Age (yr)	Error Bar (yr)	^{14}C Cal. Age (1σ)
SacA 19510	14.5	*G. ruber* + *G. sacculifer*	1,350	±30	832 (718–929)
SacA 19511	181.5	*G. ruber* + *G. sacculifer*	9,310	±30	10,079 (9,905–10,194)
SacA 19512	341.5	*G. ruber* + *G. sacculifer*	14,705	±50	17,320 (17,004–17,630)
SacA 19513	561.5	*G. ruber* + *G. sacculifer*	19,580	±70	22,778 (22,415–23,269)
SacA 19514	863.5	*G. ruber* + *G. sacculifer*	29,290	±180	33,322 (32,760–34,231)

[a]Calendar (cal.) ages were calculated and corrected from reservoir effects using the global ocean average ~400 years adjusted with a local correction 70 ± 70 years Δ*R* factor (see text for further explanations).

4. Results

4.1. Age Model Development

The shallowest core (MD01-2378) has a robust age model [*Holbourn et al.*, 2005], which is based upon (i) 20 accelerator mass spectrometry (AMS) ^{14}C dates over the last ~30 ka interval (upper ~590 cm) and (ii) the graphical correlation of its benthic δ^{18}O record to reference climatic records (e.g., the Byrd ice core for the 30–60 ka interval and the benthic stack of *Martinson et al.* [1987] for the interval 60–250 ka). Due to the robustness of its age model, we decided to use core MD01-2378 as our reference record. In order to compare properly the carbonate and organic carbon records obtained along the Timor Sea depth transect, the records should be as perfectly synchronized as possible. Using the planktonic δ^{18}O records alone did not provide enough solid tie points over several intervals characterized by low-amplitude changes. We have made the assumption therefore that since the three cores had been recovered in a narrow geographical area, striking visual similarities between the δ^{13}C, TOC, or $CaCO_3$ curves of the three cores should correspond to synchronous changes and could be tied together, using core MD01-2378 as our reference age model. The AnalySeries software [*Paillard et al.*, 1996] makes it possible to tie up graphically two records using tie points obtained from several proxy curves. The improved tuning does not modify the spectral signature of the TOC and $CaCO_3$ records compared to age models developed using the planktonic δ^{18}O records alone.

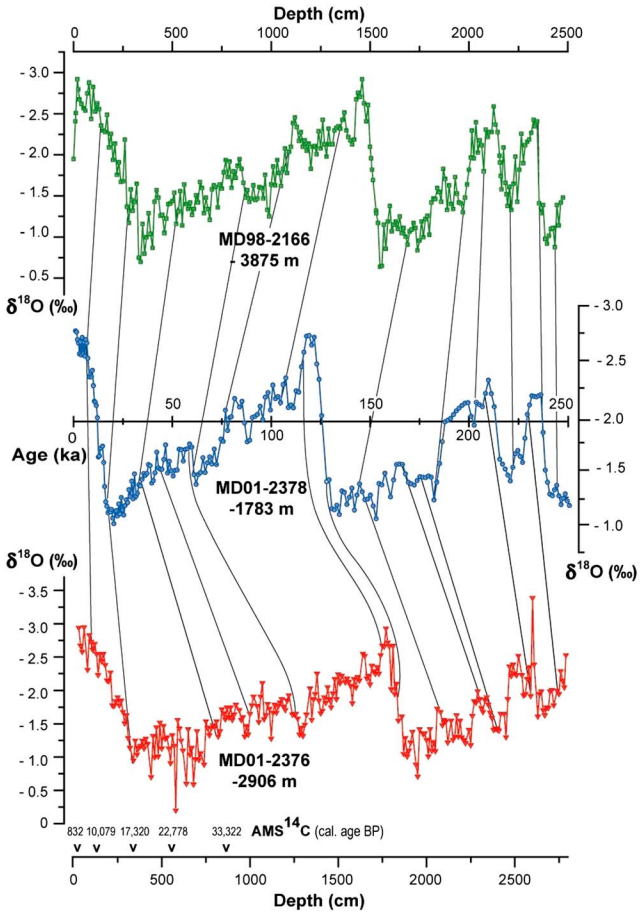

Figure 2. Planktonic oxygen isotopic record versus depth in core MD01-2376 and location of the five AMS ^{14}C dating (see Table 1). The studied core was correlated with the planktonic δ^{18}O record of the neighbor core MD01-2378 [*Holbourn et al.*, 2005]. The previously published age model of core MD98-2166 [*Moreno et al.*, 2008] was revised using core MD01-2378 as reference. Solid lines join the tie points used for correlation.

The isotopic record of the new core MD01-2376 indicates that the sediment series reaches marine isotopic stage 7.4. The five ^{14}C ages span between 0.8 ka to 33.3 cal ka B.P. (Table 1). For older part of the record, beyond ^{14}C dating, the chronology was first developed through the graphical correlation of the δ^{18}O curve to that of shallow core MD01-2378 [*Holbourn et al.*, 2005] using the linage tool of the AnalySeries software [*Paillard et al.*, 1996]. Then, as already indicated above, the correlation was refined using δ^{13}C, $CaCO_3$,

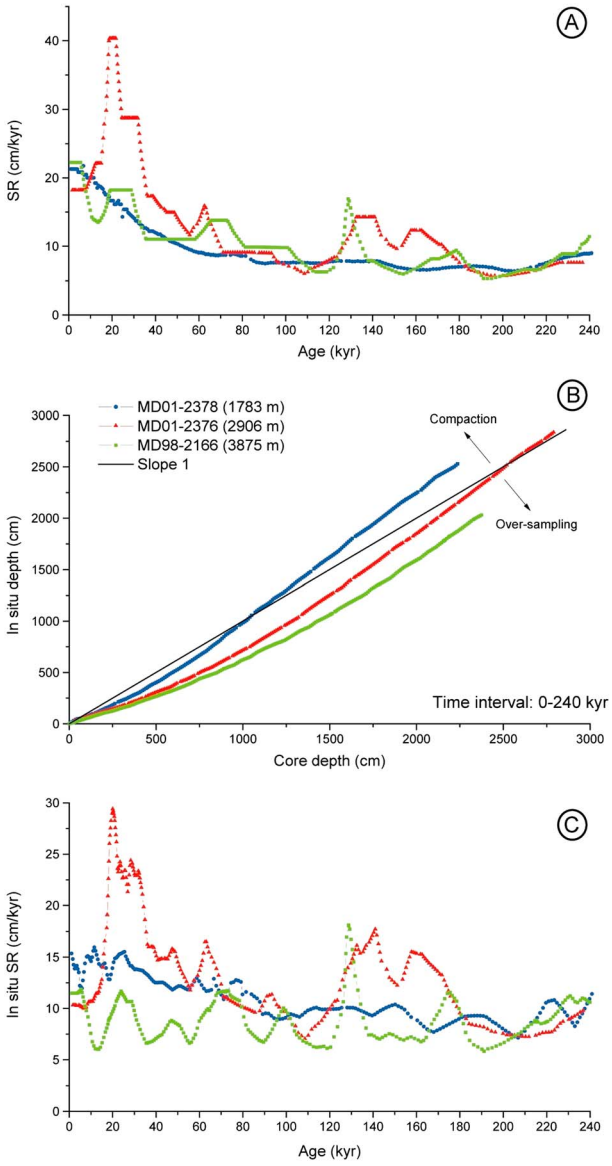

Figure 3. (a) Sedimentation rate variations along the three studied cores using the original core depth. (b) Assessment of coring disturbances (oversampling/compaction effects) of the three studied cores using the Cinema v3.0 software [*Woerther and Bourillet*, 2005; *Bourillet et al.*, 2007]. (c) Sedimentation rate variations along the three studied cores using the in situ depth estimated by the Cinema software.

and TOC curves, and the final graphic correlation rests upon 12 carefully selected tie points (Figure 2), mainly located at well-defined changes in the proxy records (rather than at peak maximum/minimum).

As far as the core MD98-2166 is concerned, an initial age model [*Moreno et al.*, 2008] had been developed based on the graphic correlation of the *G. ruber* $\delta^{18}O$ record to the isotopic record of core MD98-2165 [*Levi*, 2003; *Waelbroeck et al.*, 2006; *Levi et al.*, 2007], located to the north of the Timor Sea, west of the Pulau Sumba Island (Figure 1a). In the present paper, however, in order to optimize our intersite comparison, we modified the previously published age model of MD98-2166 to insure the highest level of synchronicity with the two other cores. Similarly, to the procedure followed for core MD01-2376, the revised age model of MD98-2166 was achieved through graphical correlation of $\delta^{18}O$, $\delta^{13}C$, $CaCO_3$, and TOC curves to those from core MD01-2378 (Figure 2).

Despite being located along a depth transect spanning nearly ~2000 m, the three cores show similar sedimentation rates, ranging from 8 to 12 cm/ka and averaging 10 cm/ka. These sedimentation rates tend to increase toward the upper part of the cores (Figure 3a). This upcore increase likely reflects an oversampling artifact associated to the elastic rebound of the coring cable when the heavy corer is released and starts to penetrate the sedimentary column [*Széréméta et al.*, 2004]. We attempted to correct this oversampling effect in the three cores using the Cinema v3.0 software developed by Institut Français de Recherche pour l'Exploitation de la Mer [*Woerther and Bourillet*, 2005; *Bourillet et al.*, 2007]. This software has been designed to model (1) the stretching and subsequent elastic rebound of the corer cable and the resulting oversampling (syringe effect) that occurs while the giant corer penetrates the upper part of the sedimentary column as well as (2) the potential under sampling (compaction) that may occur at deeper depths in the sedimentary column when increasing friction of the sediment along the core liner makes it difficult for the corer to operate correctly. The Cinema software has been parameterized based on several coring experiments achieved with a CALYPSO giant piston corer equipped with accelerometers, which made it possible to reconstruct in detail the cinematic of the coring operations. Coring behavior as modeled in Cinema is a function of the cable elastic rebound (and thus water depth) and the settings of the corer (length, weight, and height of the free fall).

The modeled, in situ depth calculated with Cinema is compared to the core depth for the three studied cores in Figure 3b. A 1:1 line (i.e., perfect recovery) is also shown for reference in the figure. The shallow core MD01-2378 shows a limited oversampling of the upper 2 m and then compaction (steeper slope than the 1:1 line). For the

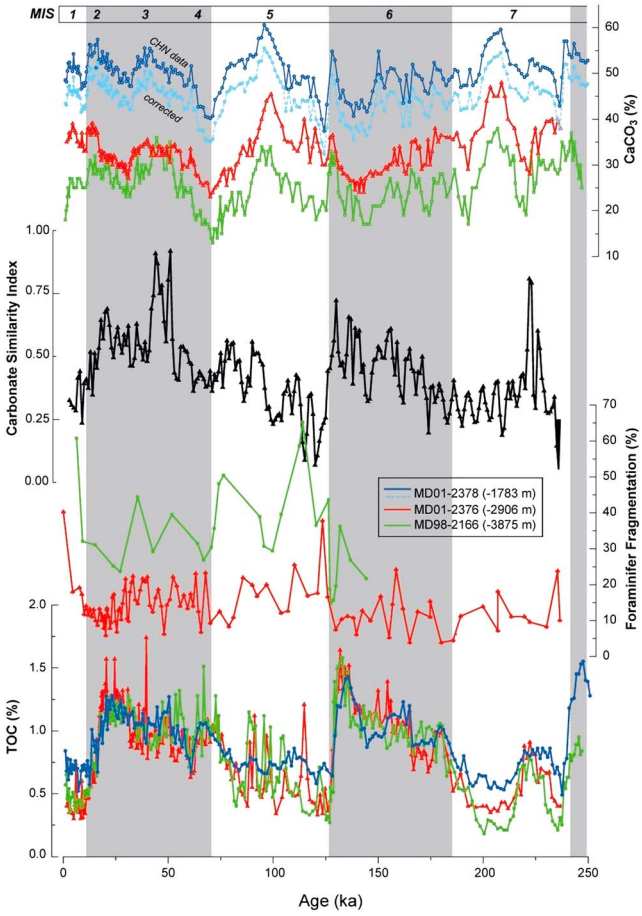

Figure 4. Comparison of $CaCO_3$ and TOC variations over the last 240 ka in the Timor Sea for the three selected cores. The corrected $CaCO_3$ curve for core MD01-2378 is due to a difference between the carbonate bomb and elemental analysis approach for $CaCO_3$ measurements. Cold episodes (marine isotope stages 2–4 and 6) correspond to the shaded areas. Data from *Holbourn et al.* [2005] for core MD01-2378 and from *Moreno et al.* [2008] for core MD98-2166. The carbonate similarity index is the interpolated ratio calculated as follows: $(CaCO_{3\ MD78} - CaCO_{3\ MD76}) / (CaCO_{3\ MD78} - CaCO_{3\ MD66})$. Foraminifer fragmentation is the proportion of foraminiferal fragments in the >150 μm size fraction.

two deepest cores, the in situ sedimentary section is likely oversampled down to about 6–7 m with a factor of about 1.5 (i.e., the upper 5 m in situ correspond to about 7.5 m in the cores). Below 6–7 m, the deepest core MD98-2166 may have recovered the sedimentary section without a slight compaction toward the end, while Cinema suggests the possibility of a stronger compaction in the lower half of core MD01-2376. Based on the Cinema results, we have estimated in situ sedimentation rates, corrected from the corer effects (Figure 3c). A clear decrease in the corrected sedimentation rate is observed on the top of the studied cores with respect to the original values. Sedimentation rates are not parallel between the records, showing less apparent intersite correlation then the TOC or $CaCO_3$ records (see below). Core MD01-2378 shows the higher sedimentation rate and also has a strong glacial-interglacial pattern with higher rates during marine isotope stage (MIS) 2 and MIS 6. The intermediate core MD01-2376 shows a more constant sedimentation rate, whereas the deepest core (MD98-2166) shows a seesaw pattern of sedimentation rate without any relationship to glacial/interglacial cycle.

The fact that sedimentation rates show a weaker apparent correlation than the TOC and $CaCO_3$ records (see below) may either suggest the importance of sediment focusing and deep current dynamics in driving the sediment accumulation at the different water depths and/or suggest that in situ depths are still biased somehow. It is important to notice that the Cinema software provides only a first-order estimate of coring disturbances, since the composition and mechanical behavior of sediments are not taken into account in the modeling of the corer penetration, leaving a potential source of uncertainties on the reconstructed in situ depths. When trying to estimate TOC or $CaCO_3$ mass accumulation rates (MARs), uncertainties on the in situ depths add up with uncertainties on the age models, on dry densities, and on the organic or inorganic carbon contents. Because of these potential uncertainties, we do not use sedimentation rates and fluxes in this paper, as we believe that the depth/age profiles are more suitable to discuss the organic carbon and carbonate records along a depth transect in the Timor Sea. A proper discussion of MAR would require that sediments had been sampled with the recent version of the CALYPSO giant corer, which is equipped with accelerometers making it possible to fully reconstruct the corer behavior. At the time of cruises IMAGES IV (MD111) and WEPAMA-IMAGES VII (MD122), this version of the corer was not yet available.

4.2. TOC and $CaCO_3$ Content

TOC values for the three cores fluctuate between ~0.2 and 1.75% (Figure 4). The TOC fluctuations show strong glacial/interglacial variations, with organic enrichment during cold periods and organic depletion during

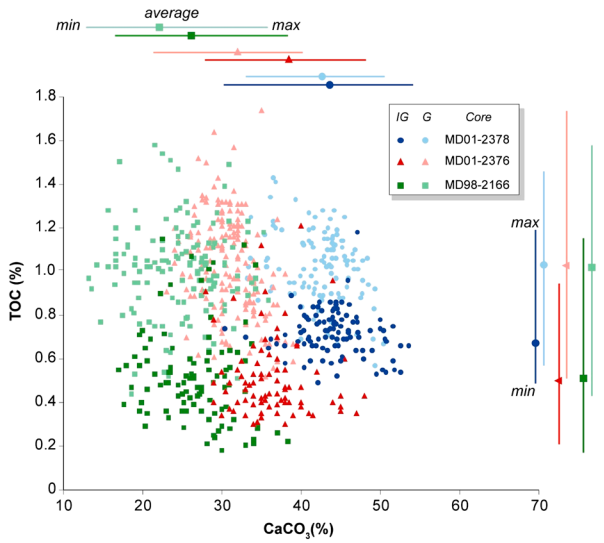

Figure 5. Organic carbon versus carbonate contents for the three selected cores (note that corrected $CaCO_3$ values are plotted for core MD01-2378) with respect to warm and cold periods. As expected, $CaCO_3$ content decreases with water depth due to carbonate dissolution. During interglacial (IG) periods, TOC content shows also a slight decrease with water depth as a consequence of the degradation of organic matter in oxic waters. During glacial (G) periods, TOC content increases and is even constant, whatever the water depth, as a result of increasing primary production and its exportation through the water column and a better preservation of organic compounds under dysoxic waters.

warm periods. Highest values are generally reached at the end of glacial stages, whereas the decreases in TOC are extremely sharp at climatic terminations. It is noteworthy that large-amplitude variations characterize the two deepest TOC records (cores MD98-2166 and MD01-2376), whereas only weak amplitude changes are observed in the shallowest TOC record (MD01-2378). This is particularly obvious in the interval MIS 5-MIS 3 (Figure 4). Values compare well between the three cores during the glacial intervals (with an average value around 1%). During interglacial intervals, however, differences exist between the three cores, with TOC values decreasing with increasing water depth (Figure 4).

The $CaCO_3$ contents show roughly parallel fluctuations with the amplitude of variations reaching ~25% in each core (Figure 4). As expected, the increase in carbonate dissolution with depth is clearly noticeable in the decrease of $CaCO_3$ values along the depth transect (i.e., values drop from 31–54% in core MD01-2378 to 13–38% in core MD98-2166). The fact that the carbonate content in core MD98-2166 reaches and even exceeds that of the shallower core MD01-2376 within marine isotope stage 3 (MIS 3), at around 50 ka (Figure 4), is a puzzling result, which clearly suggests that the differences in $\%CaCO_3$ between the three sites does not depend solely upon the increasing dissolution at depth.

$CaCO_3$ maxima are found in MIS 5 (~100 ka) and MIS 7 (~210 ka, Figure 4). Contrary to the TOC records, which show a strong seesaw evolution, temporal fluctuations in the $CaCO_3$ records do not show any long-term, glacial-interglacial pattern (Figure 4). Adjacent glacial and interglacial stages are usually separated by low or high $CaCO_3$ events, which make it possible to separate them visually, but the mean value and range of fluctuations are very similar, showing only a small decrease of glacial mean carbonate content for the two deepest sites. Such strong glacial/interglacial (G/IG) contrasts in TOC and weak differences in $CaCO_3$ are readily seen in the distribution of data when plotted on a TOC versus $CaCO_3$ graph (Figure 5).

4.3. Spectral Analysis

Spectral analysis shows dominant periodicities centered on the 100, 41, and 23 ka bands (Figure 6). As expected from the simple visual inspection, the $CaCO_3$ records only show a weak eccentricity-related glacial/interglacial signal (100 ka, Figure 6). The precession signal is only observed as a peak centered on 19 ka in the $CaCO_3$ record from core MD01-2378 (i.e., no 23 ka oscillation) and is absent from the $CaCO_3$ records of the two deepest cores. The obliquity period (41 ka) is clearly expressed in the carbonate content of the two deepest cores, whereas it is not significant in the shallowest core MD01-2378 (Figure 6).

Spectral analysis shows that the eccentricity imprint is strong in the TOC records of the three cores. However, the relative contribution of the obliquity and the precession signals changes as the function of water depth. The obliquity signal increases with increasing water depth, whereas the reverse is observed for the precession contribution, which decreases with increasing water depth.

As the three cores have relatively high sedimentation rates and were sampled with a similar temporal resolution, these depth-related differences in the power spectral of $CaCO_3$ and TOC records do not reflect aliasing problems but suggest the influence of water depth on both TOC and $CaCO_3$ preservation. It should

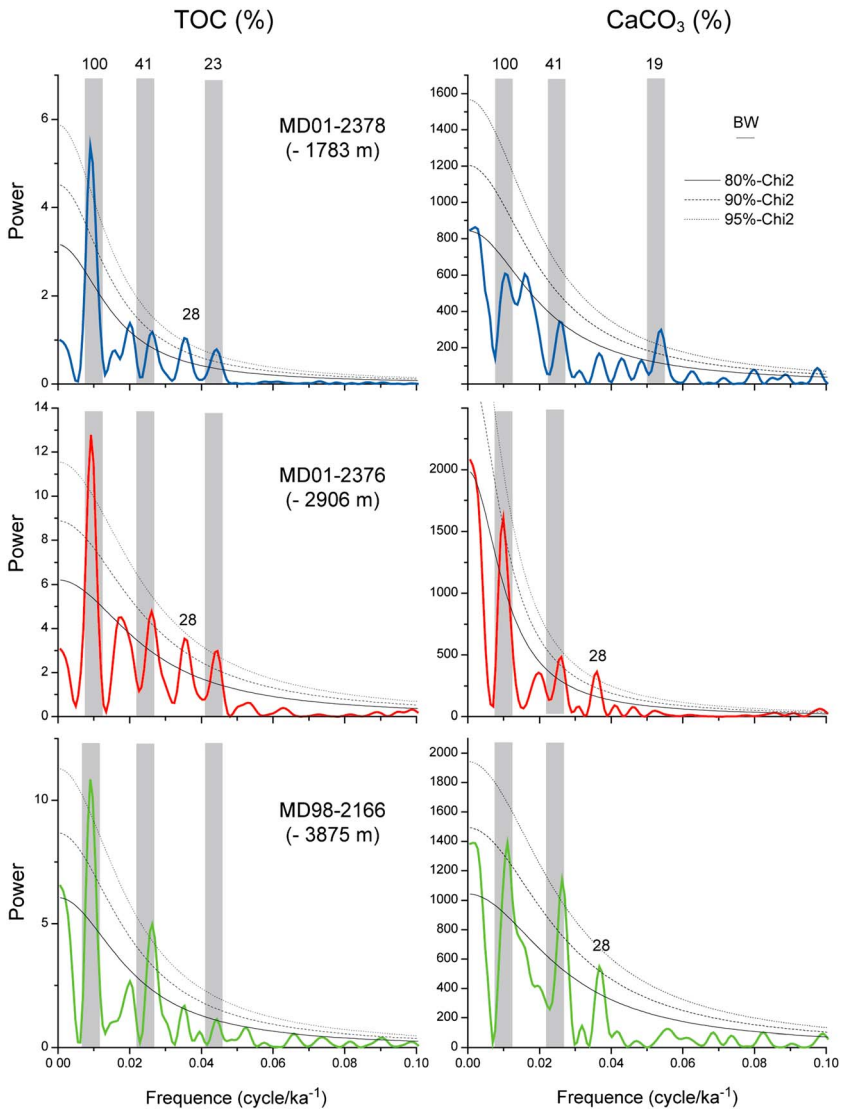

Figure 6. RedFit spectral analysis for the TOC and $CaCO_3$ records on the three selected cores for the last 240 ka.

be noted that the power spectrum obtained for the TOC record in core MD1-2378 is slightly different from that previously published by *Holbourn et al.* [2005]. This is due to the fact that in the present work, we have performed the spectral analysis over the last 240 ka only. It should also be noted that the use of a new age model for core MD98-2166 does not change the power spectrum obtain for $CaCO_3$ and TOC records by *Moreno et al.* [2008].

In addition to Milankovitch frequencies, the spectral analysis of $CaCO_3$ and TOC indicates another significant frequency at 28 ka (Figure 6), which is close to the 29–30 ka cycle observed in many low-latitude marine records [*Pisias and Rea*, 1988; *Bassinot et al.*, 1994; *Holbourn et al.*, 2005].

5. Discussion

The composition of pelagic sediments is controlled by several factors including (1) the amount of primary productivity exported below the photic zone, (2) the nature of producers (calcareous, siliceous, or organics), (3) the quantity of terrigenous particles delivered by eolian and riverine inputs, and (4) the preservation or, on the contrary, the gradual disappearance of the biogenic components during settling through the water column or at the sea bottom (i.e., dissolution of minerals and oxidation of organic matter). It is important to note that carbonate preservation/dissolution is related both to bottom water chemistry (saturation with

respect to the carbonate ions) and to the metabolic release of CO_2 into sediment pore waters during organic matter mineralization [*Emerson and Bender*, 1981]. All these factors should be considered when interpreting our results, even if it is difficult to quantify any single one independently from others.

5.1. Preservation of TOC Signal During Burial

In nearby core MD01-2379 retrieved at 560 m of water depth (see location on Figure 1a), *Gupta and Kawahata* [2006] have shown that TOC decrease with depth of burial. These authors suggested that this progressive decrease of TOC results from the continuous degradation of organic matter along burial history. In the three cores studied in the present paper, however, the TOC content is low (1% in average), and there is no noticeable decreasing trend of TOC with depth/time, even in core MD01-2378, which is the longest core (>40 m) and spans the longest time interval (450 ka) [*Holbourn et al.*, 2005]. This lack of TOC evolution suggests that the sedimented organic matter was more refractory at our three sites (i.e., had a lesser ability to be oxidized or recycled by microorganisms). The organic matter at site MD01-2379, at only 560 m of water depth, is subject to a lesser degradation during its settling through the water column than the organic matter reaching our three sites, which range from 1800 to 3900 m in depth. In addition, site MD01-2379 lies within the present-day oxygen minimum zone (OMZ). The combination of a shallow depth of deposition within the OMZ prevented extensive oxidation of the organic matter during its sedimentation, making it possible for labile organic matter to be preserved and evolve progressively through burial at the shallow site MD01-2379. In contrast at our three sites, which are deeper and not located in the OMZ, more of the labile fraction had been already consumed during settling explaining the lack of long-term, decreasing trend in TOC within the sedimentary column.

5.2. TOC Records: Primary Productivity and Preservation at the Seafloor

Optical examination of palynofacies on core MD01-2376 [*Liu*, 2011] revealed that the volumetric proportion of amorphous organic particles ranges between 90 and 98% of the total organic fraction. This is similar to the palynofacies observed at site MD98-2166 [*Moreno et al.*, 2008]. This amorphous organic matter chiefly derives from a marine source as indicated by $\delta^{13}C$ measurements of organic matter, which range between −19 and −20.5‰ [*Liu*, 2011]. As the TOC fluctuations are similar between the three sites, it is likely that the conclusions drawn from the intermediate site MD01-2376 also apply for the two other sites. We conclude therefore that TOC fluctuations along our depth transect chiefly represent changes in the production and/or preservation of marine organic matter. The remaining of the organic fraction derives from terrestrial sources and is mainly composed of wood debris, spores, and pollen grains. Although minor, the proportion of this terrestrial fraction in core MD01-2376 fluctuates along glacial-interglacial cycles as it was observed in cores MD01-2378 [*Kawamura et al.*, 2006] and MD98-2166 [*Moreno et al.*, 2008], with a slight increase of terrestrial organic matter during glacial periods. The glacial increase in terrestrial organic debris might be explained by a combination of (i) drier conditions, which promoted changes in the vegetation cover and (ii) lower sea level, which reduced the transport distance between the continent and the Timor Sea sites.

TOC values are surprisingly similar at all sites during glacial periods (Figure 4). During interglacial periods, however, TOC values decrease along the depth transect, resulting in clear offsets between the three TOC records (Figure 4). This is particularly apparent at the beginning and end of MIS 7, at the beginning of MIS 5 and—although less clear—during MIS 1 (Figure 4). Since carbonate content decreases along the depth transect, this decrease of TOC with depth cannot be attributed to an increasing dilution effect by carbonates. In addition, as shown in Figure 4, the organic carbon content largely fluctuates independently of the carbonate content, both during glacial and interglacial periods.

Assuming that the primary flux of TOC leaving the photic zone was similar at these three nearby sites, the depth-related difference in TOC content between the sites could indicate a stronger degradation of organic matter along the transect at the beginning of MIS 7, MIS 5, and MIS 1, and at the end of MIS 7. This suggests a stronger ventilation of the intermediate and deep waters during these periods.

By contrast, during glacial periods and cold stadials of MIS 5, the TOC percentage increases, and there is no noticeable difference between the three studied sites (Figure 4). The higher TOC values result in part from increased export productivity, associated to increased surface water mixing [*Holbourn et al.*, 2005; *Xu et al.*, 2006, 2008]. In addition, the fact that the relative proportion of TOC is similar between the three sites suggests also a lesser ventilation (sluggish circulation) and reduction in the oxygen content at intermediate

and deepwater depths in the Timor Sea. This reduction in oxygen availability within the water column limited the remineralization of labile organic matter during its settling, reducing the effect of water depth on the TOC flux that deposited along the transect.

These results are in agreement with a previous study based on the comparison of benthic $\delta^{13}C$ profiles in the Timor Strait [*Holbourn et al.*, 2011], which showed that during glacial periods, the water column became more stratified, with a reduced ventilation of the deep part of the transect (lower benthic $\delta^{13}C$) relative to the interglacial stages. *Holbourn et al.* [2011] suggested that glacial/interglacial changes in $\delta^{13}C$ records and ventilation reflect major changes in the thermohaline circulation with important slowdown of the deepwater masses in the eastern Indian Ocean and Timor Sea during glacials.

5.3. $CaCO_3$ Records: Productivity and Dissolution Changes

The $\%CaCO_3$ may reflect changes in dilution by noncarbonate, biogenic, or terrigenous materials. The relative changes of $CaCO_3$ with respect to the terrigenous material can be derived from XRF-Ca/Ti ratio, where the XRF-Ti record represents the clay content [*Moreno et al.*, 2013]. The Ca/Ti ratio fluctuates parallel to the $CaCO_3$ and the XRF-Ca records, whereas the XRF-Ti record varies independently. In addition, the XRF-Ca and XRF-Ti records are not anticorrelated. These observations suggest that the dilution by terrigenous content material does not play a major role in driving $\%CaCO_3$. Thus, we suggest that higher (lower) $CaCO_3$ content reflects an increase (decrease) in carbonate production/preservation rather than a lower (higher) supply of detrital material.

Geochemical ($\delta^{13}C$, chlorine concentration) and paleontological (foraminifera, dinocysts) records have suggested that glacial surface water productivity was elevated in the Timor Sea and the eastern Indian Ocean relative to modern values [*McCorkle et al.*, 1994; *Müller and Opdyke*, 2000; *Holbourn et al.*, 2005; *Kawamura et al.*, 2006]. Changes in productivity likely explain part of the in-phase oscillations in the three $CaCO_3$ records. Spectral analyses show that the glacial/interglacial (~100 ka) pattern is only well expressed in the two deepest sites. But since the records only spans 240 ka and contain two such cycles, the lack of a stronger eccentricity-related signal may not be surprising. The most striking feature is the strong development of the ~41 ka (obliquity) signal on the three sites, whereas precession is only clearly apparent in the shallowest site. The obliquity periods, being better expressed in core MD01-2376 than in the deepest core MD98-2166, may suggest either that a strong high-latitude signal is carried out through changes in deepwater properties and/or changes in the extent of specific water masses. The study of core MD98-2166 [*Moreno et al.*, 2008] has demonstrated that the $CaCO_3$ record reflects an influence of processes controlled at high latitude (obliquity signal is dominant over precessional signals), whereas sedimentary records of core MD01-2378 show a clear tropical response [*Holbourn et al.*, 2005]. The new results on core MD01-2376, retrieved at an intermediate depth, confirm that the $CaCO_3$ record at 2900 m depth is also influenced by high-latitude forcing. In addition, rapid decoupled shifts take place in the deepest site (MD98-2166) during MIS 6, 4, and 3 (Figure 4). These shifts either correspond to abnormally low calcium carbonate contents or, during the MIS 3, to a rapid increase in $CaCO_3$ with values that reach and exceed those of intermediate core MD01-2376.

Because the three studied cores are very close, the pelagic carbonate productivity should have been similar between the sites. Thus, the differences between the $CaCO_3$ records should chiefly reflect differences in dissolution at the seafloor. This difference may evolve through time, in relation to (i) the saturation of bottom waters respective to calcite at each site and (ii) the changes in the metabolic release of CO_2 into sediment pore waters during early diagenesis [e.g., *Emerson and Bender*, 1981]. In order to compare more easily the relative evolution of $CaCO_3$ at the three sites, we computed a "relative carbonate similarity index" (Figure 4). We interpolated the three $CaCO_3$ records at a constant 1 ka increment and estimated at each level the ratio $(CaCO_{3\ MD78}–CaCO_{3\ MD76})/(CaCO_{3\ MD78}–CaCO_{3\ MD66})$. The interpretation of this relative carbonate similarity index rests upon the assumptions that (i) dissolution is minimal at the shallowest site (MD01-2378), that (ii) the initial $CaCO_3$ export flux was always similar at the three sites due to their nearby geographical location, and that (iii) differences in buried $CaCO_3$ mainly result from differences in dissolution. Based on these assumptions, the index provides the relative amount of dissolution that the middle site (MD01-2376) has experienced with respect to the total amount of percentage of carbonate loss experienced along the full transect, between the shallowest (MD01-2378) and the deepest (MD98-2166) sites.

The similarity index (SI) (Figure 4) provides some clues about the evolution of the vertical gradient of dissolution along the depth transect and is likely related therefore to the position of the lysocline. Its value tends toward zero when dissolution chiefly affected the deepest site with minor effect on the intermediate site (i.e., deep lysocline), and its value tends toward one when the middle site experienced nearly as much dissolution as the deepest site (i.e., shallower lysocline). This SI record shows a clear glacial/interglacial signal. Lower SI values during MIS 1, MIS 5, and to a lesser extent MIS 7 suggest that dissolution took place mostly at the deepest site during interglacial periods (i.e., deep lysocline). On the contrary, during glacial periods, the higher SI values suggest that the intermediate and deep sites experienced similar dissolution effects (i.e., shallow lysocline).

It is important to emphasize that SI does not provide information about the "absolute" amount of dissolution experienced along the depth transect, but it provides information about the relative difference of $\%CaCO_3$ that could be attributed to the dissolution gradient between the sites. Foraminifer fragmentation, a dissolution proxy, has been analyzed in core MD98-2166 [*Moreno et al.*, 2008] and core MD98-2176 (this study, Figure 4). Interestingly, fragmentation records are higher during peak interglacials, when SI values are low and suggest that the lysocline was deep (i.e., similar $\%CaCO_3$ of the two upper sites, whereas the deeper site shows significantly lower values). On the opposite, foraminifer fragmentation suggests low dissolution intensity at the two deepest sites during glacial maxima, when the high SI values suggest a shallow lysocline. Thus, apparently, the contrast in $\%CaCO_3$ between the sites, interpreted as indicating changes in geometry of the lysocline, does not correlate necessarily with the intensity of dissolution itself as observed from the foraminifer fragmentation. This potential decoupling may point out the fact that foraminifer fragmentation and/or the depth gradient in sediment $\%CaCO_3$ are imperfect proxies of dissolution and are potentially biased by other processes. But the decoupling may also result from the fact that dissolution at depth, within the sediments, does not only depend upon the saturation of the bottom water with respect to carbonates but is also driven by the decay of organic carbon within the sediments, which sets the final undersaturation of the interstitial water.

Interestingly, the similarity index (SI) shows a striking resemblance with the TOC records (Figure 4). This suggests that the supply of organic matter seems to play an important role in shaping the past changes of the dissolution gradients along the Timor Sea depth transect. Taken at face value, this indicates that higher (lower) TOC supplies were associated to increased (decreased) dissolution level of the middle site relative to the upper reference site. This could be related to the well-known effect of in situ metabolic CO_2 production on the saturation of pore waters relative to calcite [*Emerson and Bender*, 1981]. But what is somewhat surprising here is that this metabolic effect does not seem to play a role on the absolute amplitude of dissolution (TOC content it somewhat inversely related to the fragmentation index at the two deepest sites) but plays a role on the relative dissolution level between the sites along the transect. Similarly, the lack of a clear covariance between TOC and the $CaCO_3$ records (Figure 4) or in the TOC versus $CaCO_3$ relationship (Figure 5) at each site clearly shows that TOC fluctuations impact the difference in $CaCO_3$ between the sites (i.e., SI) but not the temporal evolution of $CaCO_3$ within a given site. Again, this suggests that the final explanation rests upon the combination of TOC supply (and its decay within the sediments) and changes in the chemistry of bottom waters (i.e., evolution of the depth profile of saturation with respect to carbonates linked to changes in water mass properties and circulation). Further studies involving a careful analysis of bottom water chemistry (e.g., B/Ca analyses of epibenthic foraminifers) will be necessary to fully unravel these puzzling results and the complexity of the dissolution mechanisms at play along the Timor transect.

6. Conclusions

The study of core MD01-2376 (2906 m of water depth) in the Timor Sea pointed out the importance of glacial/interglacial changes in the sedimentary records of carbonate and organic carbon. The comparison with previous studies performed on nearby cores MD01-2378, collected at a shallower depth (1783 m) [*Holbourn et al.*, 2005], and MD98-2166 (3875 m) [*Moreno et al.*, 2008], provides a depth transect suitable to reconstruct the impact of productivity fluctuations and water ventilation on the biogenic carbon and carbonate sedimentation within the Timor Sea for the last 240 ka.

TOC contents are similar for the three cores with values ranging from 0.2 to 1.75%, with marine organic matter enrichment during cold periods and organic matter depletion during warm periods. Highest values

are generally reached at the end of glacial stages, whereas the decreases in TOC are extremely sharp during terminations. Increase in the TOC content during glacial periods probably reflects an increase in primary productivity and a lesser decomposition of organic matter with depth due to a stronger stratification. These results are in agreement with the study of deepwater ventilation from the eastern Indian Ocean and Timor area based on benthic $\delta^{13}C$ [*Holbourn et al*., 2013].

The in-phase oscillations in the three $CaCO_3$ records reflect changes in surface productivity rather than changes in terrigenous input. Spectral analyses show that the glacial/interglacial (~100 ka) pattern is only well expressed in the two deepest sites. On the three sites, the most striking feature is the strong development of the ~41 ka (obliquity) signal, whereas precession is only clearly apparent in the shallowest site. This suggests the influence of the deep waters (possibly the Circumpolar Deep Water) in transmitting a high-latitude signal, which impact the TOC and $CaCO_3$ contents in the deep Timor Sea.

Acknowledgments

Cores were collected during IMAGES cruise IPHISII and IMAGES cruise WEPAMA onboard the R/V *Marion Dufresne*. Thanks are due to the IPEV team and the crew of the R/V *Marion Dufresne* for their support during these cruises. Technical assistance in organic matter and carbonate measurements was provided by Florence Savignac and Anne-Marie Brunet, whereas Alexandre Lethiers helps us to produce figures. We are indebted to Pierre-Jean Giannesini for his help in smear slide observation. Cores MD01-2376 and MD98-2166 are stored in the marine collection from the Natural History Museum from Paris. This is reference work 5312 of LSCE.

References

Antoine, D., J.-M. André, and A. Morel (1996), Oceanic primary production: 2. Estimation at global scale from satellite (Coastal Zone Color Scanner) chlorophyll, *Global Biogeochem. Cycles*, *10*(1), 57–69, doi:10.1029/95GB02832.

Bassinot, F., L. Labeyrie, E. Vincent, X. Quidelleur, N. J. Shackleton, and Y. Lancelot (1994), The astronomical theory of climate and the age of the Brunhes-Matuyama magnetic reversal, *Earth Planet. Change*, *126*(1–3), 91–108.

Bourillet, J.F., G. Damy, L. Dussud, N. Sultan, P. Woerther, and S. Migeon (2007), Behaviour of a piston corer from accelerometers and new insights on quality of the recovery, Proceedings of the Sixth International Offshore Site Investigation and Geotechnics Conference: Confronting New Challenges and Sharing Knowledge, 11–13 September, 2007, London, U. K.

Bray, N. A., S. Hautala, J. Chong, and J. Pariwono (1996), Large-scale sea level, thermocline, and wind variations in the Indonesian throughflow region, *J. Geophys. Res.*, *101*(C5), 12,239–12,254, doi:10.1029/96JC00080.

Coplen, T. B. (1988), Normalization of oxygen and hydrogen isotope data, *Chem. Geol. (Isotope Geoscience Section)*, *72*, 293–297.

Dunn, D. A. (1980), Revised techniques for quantitative calcium carbonate analysis using the "Karbonat-Bombe" and comparisons to other quantitative carbonate analysis methods, *J. Sediment. Petrol.*, *50*, 630–637.

Emerson, S., and M. L. Bender (1981), Carbon fluxes at the sediment-water interface of the deep-sea: Calcium carbonate preservation, *J. Mar. Res.*, *39*, 139–162.

Fieux, M., C. Andrié, P. Delecluse, A. G. Ilahude, A. Kartavtseff, F. Mantisi, R. Molcard, and J. C. Swallow (1994), Measurements within the Pacific-Indian oceans throughflow region, *Deep Sea Res., Part I*, *41*(7), 1091–1130.

Gagan, M. K., E. J. Hendy, S. G. Haberle, and W. S. Hantoro (2004), Post-glacial evolution of the Indo-Pacific Warm Pool and El Niño-Southern oscillation, *Quat. Int.*, *118–119*, 127–143.

Gordon, A. L., J. Sprintall, H. M. Van Aken, D. Susanto, S. Wijffels, R. Molcard, A. Ffield, W. Pranowo, and S. Wirasantosa (2010), The Indonesian throughflow during 2004–2006 as observed by the INSTANT program, *Dyn. Atmos. Oceans*, *50*(2), 115–128.

Gupta, L. P., and H. Kawahata (2006), Downcore diagenetic changes in organic matter and implications for paleoproductivity estimates, *Global Planet. Change*, *53*(1–2), 122–136.

Hirst, A. C., and J. S. Godfrey (1993), The Role of Indonesian Throughflow in a Global Ocean GCM, *J. Phys. Oceanogr.*, *23*(6), 1057–1086.

Holbourn, A., W. Kuhnt, H. Kawamura, Z. Jian, P. Grootes, H. Erlenkeuser, and J. Xu (2005), Orbitally paced paleoproductivity variations in the Timor Sea and Indonesian Throughflow variability during the last 460 kyr, *Paleoceanography*, *20*, PA3002, doi:10.1029/2004PA001094.

Holbourn, A., W. Kuhnt, and J. Xu (2011), Indonesian Throughflow variability during the last 140 ka: The Timor Sea outflow, *Geol. Soc. London Spec. Publ.*, *2011*(355), 283–303.

Kawamura, H., A. Holbourn, and W. Kuhnt (2006), Climate variability and land-ocean interactions in the Indo Pacific Warm Pool: A 460-ka palynological and organic geochemical record from the Timor Sea, *Mar. Micropaleontol.*, *59*(1), 1–14.

Kershaw, A. P., S. van der Kaars, and P. T. Moss (2003), Late Quaternary Milankovitch-scale climatic change and variability and its impact on monsoonal Australasia, *Mar. Geol.*, *201*(1–3), 81–95.

Kuhnt, W., A. Holbourn, R. Hall, M. Zuvela, and R. Käse (2004), Neogene history of the Indonesian Throughflow, in *Continent-Ocean Interactions Within East Asian Marginal Seas*, *Geophys. Monogr. Ser.*, vol. 149, edited by P. Clift et al., pp. 287–308, AGU, Washington, D. C.

Le, J., and N. J. Shackleton (1992), Carbonate dissolution fluctuations in the Western Equatorial Pacific during the late Quaternary, *Paleoceanography*, *7*, 21–42, doi:10.1029/91PA02854.

Levi, C. (2003), Étude des variations climatiques de la zone Indo-Pacifique: Rôle des basses latitudes dans la variabilité millénaire du climat, PhD thesis, Université Paris-11, Orsay, France.

Levi, C., L. Labeyrie, F. Bassinot, F. Guichard, E. Cortijo, C. Waelbroeck, N. Caillon, J. Duprat, T. de Garidel-Thoron, and H. Elderfield (2007), Low-latitude hydrological cycle and rapid climate changes during the last deglaciation, *Geochem. Geophys. Geosyst.*, *8*, Q05N12, doi:10.1029/2006GC001514.

Liu, W. (2011), Influence de la mousson et des changements du nibveau marin sur la sédimentation hémipélagique en Mer de Timor au cours des derniers 240 ka, PhD thesis, UPMC, Paris, France.

Martinson, D. G., N. G. Pisias, J. D. Hays, J. Imbrie, T. C. Moore, and N. J. Shackleton (1987), Age dating and the orbital theory of the ice ages: Development of a high- resolution 0 to 300.000 year chronostratigraphy, *Quat. Res.*, *27*, 1–29.

Matsumoto, J. (1992), The seasonal changes in Asian and Australian monsoon regions, *J. Meteorol. Soc. Jpn.*, *70*(1B), 257–273.

McCorkle, D. C., H. H. Veeh, and D. T. Heggie (1994), Glacial-Holocene Paleoproductivity off Western Australia: A Comparison of Proxy Records, in *Carbon Cycling in the Glacial Ocean: Constraints on the Ocean's Role in Global Change*, edited by R. Zahn et al., pp. 443–479, Springer, Berlin Heidelberg.

McPhaden, M. J., and J. Picaut (1990), El Niño-Southern Oscillation Displacements of the Western Equatorial Pacific Warm Pool, *Science*, *250*(4986), 1385–1388.

Moreno, E., F. Bassinot, F. Baudin, and M.-T. Vénec-Peyré (2008), Influence of orbital forcing and sea level changes on sedimentation patterns in the Timor Sea during the last 260 ka, *Paleoceanography*, *23*, PA1207, doi:10.1029/2007PA001423.

Moreno, E., W. Liu, F. Baudin, N. Fang, and F. Bassinot (2013), Monsoon and sea level changes in the control of terrigenous inputs and paleoproductivity in the Timor Sea during the past 240 kyr, 11th International Conference on Paleoceanography, Sitges, Spain.

Müller, A., and B. N. Opdyke (2000), Glacial- interglacial changes in nutrient utilization and paleoproductivity in the Indonesian Throughflow sensitive Timor Trough, easternmost Indian Ocean, *Paleoceanography*, *15*(1), 85–94, doi:10.1029/1999PA900046.

Murgese, D. S., and P. De Deckker (2005), The distribution of deep-sea benthic foraminifera in core tops from the eastern Indian Ocean, *Mar. Micropaleontol.*, *56*(1–2), 25–49.

O'Connor, S., S. Ulm, S. J. Fallon, A. Barham, and I. Loch (2010), Pre-bomb marine reservoir variability in the Kimberley region, Western Australia. Radiocarbon, *Radiocarbon*, *52*(2–3), 1158–1165.

Paillard, D., L. Labeyrie, and P. Yiou (1996), Macintosh program performs time-series analysis, *EOS Trans.*, *77*, 379.

Pisias, N. G., and D. K. Rea (1988), Late Pleistocene paleoclimatology of the central equatorial Pacific: Sea surface response to the southeast Trade Winds, *Paleoceanography*, *3*(1), 21–37, doi:10.1029/PA003i001p00021.

Ramage, C. S. (1968), Role of a tropical "maritime continent" in the atmospheric circulation, *Mon. Weather Rev.*, *96*(6), 365–370.

Schulz, M., and M. Mudelsee (2002), REDFIT: Estimating red-noise spectra directly from unevenly spaced paleoclimatic time series, *Comput. Geosci.*, *28*(3), 421–426.

Sprintall, J., S. E. Wijffels, R. Molcard, and I. Jaya (2009), Direct estimates of the Indonesian Throughflow entering the Indian Ocean: 2004–2006, *J. Geophys. Res.*, *114*, C07001, doi:10.1029/2008JC005257.

Stuiver, M., and T. F. Braziunas (1993), 14C ages of marine samples to 10,000 BC, *Radiocarbon*, *35*(1), 137–189.

Stuiver, M., P. J. Reimer, and T. F. Braziunas (1998), High-precision radiocarbon age calibration for terrestrial and marine samples, *Radiocarbon*, *40*(3), 1127–1151.

Széréméta, N., F. Bassinot, Y. Balut, L. D. Labeyrie, and M. Pagel (2004), Oversampling of sedimentary series collected by giant piston corer: Evidence and corrections based on 3.5 kHz chirp profiles, *Paleoceanography*, *19*, PA1005, doi:10.1029/2002PA000795.

Tapper, N. (2002), Climate, climatic variability and atmospheric circulation patterns in the Maritime Continent region, in *Bridging Wallace's Line: The Environmental and Cultural History and Dynamics of the SE-Asian-Australian Region*, Adv. Geoecol., vol. 34, edited by A. P. Kershaw et al., pp. 5–28, Catena Verlag, Reiskirchen.

Thunell, R. C. (1976), Calcium carbonate dissolution history in late Quaternary deep-sea sediments, Western Gulf of Mexico, *J. Quat. Res.*, *6*, 281–297.

Waelbroeck, C., C. Levi, J. C. Duplessy, L. Labeyrie, E. Michel, E. Cortijo, F. Bassinot, and F. Guichard (2006), Distant origin of circulation changes in the Indian Ocean during the last deglaciation, *Earth Planet. change*, *243*(1–2), 244–251.

Wang, B., I. S. Kang, and J. Y. Lee (2004), Ensemble Simulations of Asian–Australian Monsoon Variability by 11 AGCMs, *J. Clim.*, *17*(4), 803–818.

Wheeler, M. C., and J. L. McBride (2005), Australian-Indonesian monsoon, in *Intraseasonal Variability in the Atmosphere–Ocean Climate System*, edited by W. K. M. Lau and D. E. Waliser, pp. 125–173, Praxis, Springer, Berlin Heidelberg.

Woerther, P., and J.F. Bourillet (2005), Exploitation des mesures faites avec les accéléromètres sur le carottier CAPYPSO - Mission SEDICAR4-ALIENOR, Ifremer, Brest, TSI/SI/06/10, pp. 47 & 4 annexes.

Xu, J., W. Kuhnt, A. Holbourn, N. Andersen, and G. Bartoli (2006), Changes in the vertical profile of the Indonesian Throughflow during Termination II: Evidence from the Timor Sea, *Paleoceanography*, *21*, PA4202, doi:10.1029/2006PA001278.

Xu, J., A. Holbourn, W. Kuhnt, Z. Jian, and H. Kawamura (2008), Changes in the thermocline structure of the Indonesian outflow during Terminations I and II, *Earth Planet. Sci. Lett.*, *273*(1–2), 152–162.

Yan, X.-H., C.-R. Ho, Q. Zheng, and V. Klemas (1992), Temperature and Size Variabilities of the Western Pacific Warm Pool, *Science*, *258*(5088), 1643–1645.

Zuraida, R., A. Holbourn, D. Nürnberg, W. Kuhnt, A. Dürkop, and A. Erichsen (2009), Evidence for Indonesian Throughflow slowdown during Heinrich events 3–5, *Paleoceanography*, *24*, PA2205, doi:10.1029/2008PA001653.